Full PAPER

Local-and regional-scale spatial patterns of two fungal pathogens of *Miscanthus sinensis* in grassland communities

*Ryo O. Suzuki

Yousuke Degawa

Sugadaira Montane Research Center, University of Tsukuba, 1278-294 Sugadaira-kogen Ueda, Nagano 386-2204, Japan

Satoshi N. Suzuki

The University of Tokyo Chichibu Forest, Graduate School of Agricultural and Life Sciences, The University of Tokyo, 1-1-49 Hinoda-machi, Chichibu, Saitama 368-0034, Japan

Tsuyoshi Hosoya

Department of Botany, National Museum of Nature and Science, 4-1-1 Amakubo, Tsukuba, Ibaraki 305-0005, Japan

Correspondence: R. O. Suzuki,

Tel.: +81-268-74-2002

Fax: +81-268-74-2016

E-mail: rsuzuki@sugadaira.tsukuba.ac.jp

Text 18 pages; Table 1; Figures 4

Abstract We studied the spatio-temporal patterns in two fungal pathogens, *Sporisorium kusanoi*, along with *Naemacyclus culmigenus*, of the Japanese pampas grass (*Miscanthus sinensis*) in grassland communities on the Sugadaira plateau, Japan. Their disease symptoms emerged early in June, increased rapidly during the month and peaked early in July. We checked their presence at 11 sites (the regional-scale census) and recorded their presence in 6000 1 × 1-m subplots within a 60 × 100-m area at the specific site (the local-scale census). *Sporisorium kusanoi* and *N. culmigenus* were observed at eight and one sites in the regional-scale census, and in 987 and 2708 subplots in the local-scale census, respectively. The respective spatial distributions of *S. kusanoi* and *N. culmigenus* aggregated at the spatial scales of 13 m and 33 m. However, the spatial positions of the two fungi were slightly repulsive each other. Our results found that *S. kusanoi* was widely distributed within the region, whereas *N. culmigenus* was restricted within the specific site but had a higher frequency compared to *S. kusanoi*. The contrasting spatial patterns of the two pathogens may reflect differences in their dispersal processes.

Keywords

Metapopulation, *Naemacyclus culmigenus*, Spatial analysis, *Sporisorium kusanoi*

1. Introduction

Investigation of the spatial patterns of plant pathogens is essential for understanding the ecological and evolutionary dynamics between plants and pathogens. In the concept of emerging infectious diseases (Anderson 2004; Desprez-Loustau et al. 2007), the invasion of a new plant pathogen in a new region can be assumed to depend on its dispersal ability. When the pathogen has low dispersal ability, its spread is limited to within the first host population invaded and a long time is required to diffuse into other host populations in the region. A pathogen with high dispersal ability can rapidly diffuse into several host populations simultaneously with its spread in the first population invaded. After invasion, the metapopulation dynamics of plant–pathogen interactions largely determine the co-existence and co-evolutionary processes. Genetic variations in resistance and virulence, the dispersal processes of the pathogen, and the spatial distribution patterns of host plants within and among populations are all crucial factors affecting the ecological and evolutionary dynamics of plant–pathogen metapopulations (Thrall and Burdon 2000, 2003; Carlsson-granér and Thrall 2002; Laine 2004). Compared to many studies on plant–pathogen metapopulation dynamics (e.g. Burdon et al. 1995; Garcia-Guzmaan et al. 1996; Thrall and Burdon 2000, 2003; Laine 2004; Laine and Hanski 2006), the initial diffusion processes of a pathogen to a new region or a new host range has rarely been studied.

For most pathogens of wild plants, the initial diffusion processes at local and regional scales are unclear. Because identifying the early stage is very difficult when the new pathogen begins to invade a new region, most outbreaks are recorded only when it has already diffused throughout a specific region. Statistical analysis of the spatial distributions of organisms can

68 be useful to infer the diffusion processes of a pathogen in situations in which it has already
69 spread throughout a habitat. Spatial pattern analysis has developed from the 1980s as a
70 statistical method used to identify the underlying factors determining the spatial dynamics of
71 plant populations, such as intra- and inter-specific interactions, environmental heterogeneity,
72 the mortality process, and seed dispersal (Sterner et al. 1986; Pélissier 1998; Barrot et al.
73 1999; Cole and Syms 1999; Dale 1999; Dovčiak et al. 2001; Debski et al. 2002; Suzuki et al.
74 2003, 2005, 2009, 2012). The application of spatial analysis to plant–pathogen dynamics has
75 also increased in recent years (Garcia-Guzmaan et al. 1996; Real and McElhany 1996; Laine
76 and Hanski 2006). Spatial analysis can help us to infer the processes of dispersal and infection
77 for new pathogens with little basic information about their life history.

78 In this study, we evaluated the spatial distribution patterns of the smut fungus
79 *Sporisorium kusanoi* (Syd. & P. Syd.) Vánky and the discomycete *Naemacyclus culmigenus*
80 Ellis & Langl. at the regional scale and at the local scale within a site, and their seasonal
81 patterns at the local site. The target fungi are observed on the Japanese pampas grass
82 *Miscanthus sinensis* at a certain abundance with remarkable symptoms, and they can be
83 therefore utilized as model organisms to evaluate the spatial dynamics of plant–pathogen
84 interactions in a region. This study reports the detailed spatio-temporal patterns of the two
85 fungal pathogens including *N. culmigenus* inhibiting a new host and new habitat.
86
87
88 **2. Materials and methods**
89
90 2.1. Study site

In this study, we investigated the spatial distribution patterns of the two fungi roughly at the regional scale and intensively at the local scale. The regional-scale census was conducted in 11 grassland sites where *M. sinensis* was distributed on the Sugadaira plateau at an altitude of about 1300 m, Ueda-shi, Nagano Prefecture, central Japan. The annual mean temperature of the plateau was 6.5°C and the average monthly temperature ranged from 19.4°C in August to –5.6°C in February, while the mean annual rainfall was 1226 mm and the average maximum snow depth was 102 cm for the period 1971–2006. The maintenance of the 11 grassland sites involved the removal of all of the above-ground plant parts during the growing season of each year and most of sites were used as ski slopes.

The local-scale census was conducted at a grassland site in the Sugadaira Montane Research Center (36°31’N, 138°21’E; hereafter, called the SMRC site). The grassland has an area of 6 ha (200 × 300 m). Every autumn for 75 years, the facilities managers have removed all of the above-ground plant parts to prevent vegetative succession from grassland to forest. *M. sinensis* dominated the site with the largest biomass. In a preliminary census, more than 100 plant species were recorded in the grassland.

2.2. Study species

We investigated fungal pathogens on the Japanese pampas grass, *M. sinensis*, which is widely distributed throughout East Asia and is common to grasslands, riversides, and abandoned fields in Japan. During the growing season, plants elongate several shoots from an underground rhizome and form a dense clump. Each shoot grows to a height of 0.5–3 m.

Flowering begins in August. Reproductive plants produce a large number of small seeds. Fruit maturation and seed dispersal occur in September–October. Following reproduction, all of the above-ground parts will have withered by the end of autumn.

At the study sites, *M. sinensis* was infected by the smut fungus, *Sporisorium kusanoi* (Ustilaginaceae, Ustilaginales, Ustilaginomycetes, Basidiomycota), along with *Naemacyclus culmigenus* (family incertae sedis, Helotiales, Leotiomycetes, Ascomycota). Smut fungi are very popular plant-pathogens causing smut-like disease symptoms (Webster and Weber 2007). It produces loose masses of dark spores in infected plant organs, and infected individuals usually cannot fruit. When *S. kusanoi* infected *M. sinensis* plants, they produced large numbers of spores in the surface of several stems of infected plants. Stems with spores cannot grow and develop reproductive organs.

Naemacyclus culmigenus is a fungus with erumpent apothecia that are assumed to cause leaf blight in *M. sinensis.* Initially it was noticed in summer 2010 at the SMRC site and was identified as a species new to Japan (Hosoya et al. 2013).

Both of the pathogens substantially decreased the growth and size of the hosts and systemically infected host plants (R. O. Suzuki and Y. Degawa, personal observation). Basic information about the life-history, dispersal, and infection processes of both pathogens in *M. sinensis* is very little. In this study, we recognized the two fungi from the visible disease symptoms on *M. sinensis* (dark stems covered with spores for *S. kusanoi* and a development of reddish zonation in the middle area of the leaf along the vein for *N. culmigenus*).

2.3. Field census

In the regional-scale census, we confirmed the presence/absence of the two fungi at 11 sites on the Sugadaira plateau in Aug 2011 (Fig. 1A). The sites were selected according to the population size of *M. sinensis* and their accessibility, without consideration of the presence of the two pathogens and environmental conditions before the census. *S. kusanoi* generally displayed patchy distribution in the study sites. We established a 16 × 16-m plot within a patch of *S. kusanoi* at each site and divided the plot into 25 grids at 4-m intervals. We counted the presence/absence of the two fungi and host plants in a 50 cm radius around each grid point. The relative frequency of fungi was calculated as the number of grid points with diseased plants divided by the number of grid points where host plants were observed.

In the local-scale census, we monitored seasonal and spatial patterns of the prevalence of the two fungi within the SMRC site (Fig. 1B). To evaluate the seasonal patterns of both pathogens, we established three 160-m transects in the grassland and placed 40 1 × 1-m plots on each transect in 2010 (120 plots in total). These transects were located at least 25 m apart from each other and plots in each transect were located 3 m apart from each other. After the snow had melted within all plots in 2011, the establishment of *M. sinensis* and the existence of the two pathogens in each plot were recorded at 3–17 d intervals from 18 Apr to 15 Jul 2011. To evaluate the spatial patterns of the prevalence of the two fungi at the local scale, we established a 60 × 100-m plot in the SMRC site. The plot was divided into 6000 1 × 1-m subplots. The presence of *M. sinensis* and the two fungi was recorded within each subplot on 28–29 Jun 2011 when the prevalence of the two pathogens was maximally observed.

2.4. Analysis

We performed out spatial autocorrelation analyses to detect spatial patches of the fungi at the local scale. The spatial autocorrelation analyses tested whether subplots that were located within defined distance ranges shared the same fungi (Sokal and Oden 1978a, b; Sakai and Oden 1983). Values of Moran's *I* were calculated for distances at 1-m intervals up to 60 m. A positive autocorrelation indicated that the fungus was spatially aggregated at the corresponding scale. We tested whether the observed values of Moran's *I* were significantly different ($P < 0.01$) from those calculated under the null hypothesis of a spatially random pathogen. The distribution of *I* values under the null hypothesis was obtained by 1000 random permutations of the data set. In this study, we considered that the minimum distance classes at which significantly positive *I* values were absent indicated the spatial scale of aggregated pathogens (the definition following Dale 1999).

The cross-correlation statistic (I_{12}) was used to test the null hypothesis of no spatial cross-correlation between *S. kusanoi* and *N. culmigenus*. Positive and negative values indicated that the two fungi were spatially attracted and segregated, respectively, at the corresponding scale. We tested whether the observed values of I_{12} were significantly different ($P < 0.01$) from those calculated under the null hypothesis of spatial independence. The distribution of I_{12} values under the null hypothesis was obtained by 1000 random permutations of the data set.

3. Results

The regional-scale census recorded *S. kusanoi* and *N. culmigenus* in eight and one sites, respectively (Table 1). Even though we established a grid-census plot within a dense patch of

183 *S. kusanoi* at each site, *S. kusanoi* at the eight sites generally had a low frequency, with
184 diseased plants observed less than 40% of the grid points where host plants were observed.
185 Seasonal patterns of the fungal prevalence at the SMRC site were similar for the two
186 pathogens (Fig. 2). Shoot elongation of *M. sinensis* was initiated at 9 May 2011 and observed
187 in 114 plots by 9 Jun. There was no *M. sinensis* plant in residual 6 plots during the study
188 period. The disease symptoms of the two fungi emerged early in June and increased rapidly
189 during the month. The emergence of symptoms peaked at the end of June for *S. kusanoi* and at
190 the beginning of July for *N. culmigenus*.
191 Spatial patterns at the SMRC site differed between the two fungi (Fig. 3). Of 5729
192 subplots (95.5%) where *M. sinensis* was established, *S. kusanoi* and *N. culmigenus* were
193 observed in 987 (17.2%) and 2708 (47.3%) subplots, respectively. Spatial autocorrelation
194 analysis demonstrated that the spatial distributions of *S. kusanoi* and *N. culmigenus* were
195 significantly aggregated at the spatial scale of 13 m and 33 m, respectively (Fig. 4A, B).
196 Cross-correlation analysis revealed that the spatial positions of the two pathogens were
197 slightly negative at a scale smaller than 40 m (Fig. 4C), and were especially significant at the
198 spatial scale of 22 m. We found no shoots showing symptoms of double infections by both
199 fungi.
200
201 **4. Discussion**
202
203 Our results revealed that *S. kusanoi* was widely distributed within the study region at each
204 local site, whereas *N. culmigenus* was restricted within a specific site with a relatively high
205 frequency compared to *S. kusanoi*. The contrasting spatial patterns of the two pathogens likely

reflect the differences in dispersal processes.

In general, infection by flower-smut fungi often causes the development of stamens that produce fungal spores. These spores are dispersed by insects visiting diseased flowers, which then transmit spores to intact flowers (Alexander and Antonovics 1988; Jennersten 1988). However, this pollinator-mediated dispersal process was unlikely to occur in our study system, in which *S. kusanoi* produced no spores in flowers but large numbers of spores in the stems of *M. sinensis*. Some other organisms, such as grasshoppers, larvae, and insect predators, utilizing the leaves and stems of *M. sinensis*, may potentially transfer spores of *S. kusanoi*. In contrast, no information is available regarding the dispersal process of *N. culmigenus*. *Cyclaneusma* DiCosmo, Peredo & Minter, a phylogenetically close genus to *Naemacyclus* has been reported to needle-cast; *Cyclaneusma minus* (synonym *Naemacyclus minor*) requires moisture to release spores that are dispersed by rain and wind (Gadgil 1984). The spatial distributions of the two fungi observed at the local scale suggest differences in dispersal mechanism between them, with diseased plants infected by *N. culmigenus* forming larger patches (33 m in diameter) than those infected by *S. kusanoi* (13 m). The formation of large patches of disease seems to be due to longer distance dispersal by rain- and wind-dispersal, whereas the small patches of disease might be caused by short distance dispersal by insect dispersal. Aerial dispersal of pathogens also potentially generates extreme long-distance dispersal on regional, continental, and global scales (Brown and Hovmøller 2002). However, the restricted distribution of *N. culmigenus* (only recorded at one site) suggests limited extreme long-distance dispersal of spores between host populations or a very short history after invasion in this region. When and how *N. culmigenus* invaded the first host population at the SMRC site are also unclear. Invasion of a new pathogen to a new

229 geographical range can be caused by artificial transportation due to human activity (Anderson
230 et al. 2004), although no evidence exists to support this possibility at our study sites.
231 The ecological dynamics of plant–pathogen interactions in natural habitats are well
232 illustrated in the context of metapopulation dynamics, which are often spatially explicit
233 (Thrall and Burdon 1997, 2003; Burdon and Thrall 1999; Laine 2004; Laine and Hanski
234 2006; Bardgett and Wardle 2010). A newly emerged pathogen with high infection ability
235 often causes an epidemic of a disease in a host population which is naive to the pathogen
236 (Daszak et al. 2000; Anderson et al. 2004; Desprez-Loustau et al. 2007). High dispersal
237 ability can allow the plant pathogen to spread rapidly among host populations and can result
238 in epidemism of the disease at regional scales. Genetic diversity in host resistance and
239 pathogen virulence also largely influence metapopulation dynamics of plant–pathogen (Thrall
240 and Burdon 2000, 2003; Laine 2004), although we had no data suggesting the genetic
241 diversity. Spatial patterns of host populations also influence pathogen incidence in such a way
242 that isolated host populations distant from other populations tend to remain free of pathogens
243 in contrast to populations close to infected populations (Burdon et al. 1989, 1997;
244 Carlsson-granér and Thrall 2002). Our results partially supported this patterns; site 6, 7, and 9
245 that were distant from other infected populations were with no or rare frequency of *S. kusanoi*
246 infection. However, the relative importance of the dispersal ability of a pathogen, genetic
247 diversity in resistance and virulence, and spatial patterns of host populations that account for
248 the metapopulation dynamics remain unclear.
249 Our results found a negative spatial association between the two fungi at the 22-m
250 scale and no observation of double infections in a host shoot. Although these segregated
251 patterns observed here were based on weak evidence, segregated patterns are often caused by

252 competitive interactions between species. Competitive interactions among plant-symbiont
253 mycorrhizal fungi have been reported (Cano and Bago 2005; Kennedy and Bruns 2005;
254 Kennedy et al. 2007, 2010; Pickles et al. 2010), relative to few studies demonstrating
255 competition among plant pathogenic fungi. However, disease symptoms of the two pathogens
256 were observed in different plant organs each other: *S. kusanoi* on stems and *N. culmigenus* on
257 leaves. Therefore, direct competitive interaction between them is unlikely to occur within a
258 single plant organ, although the pathogens might potentially inhabit within all organs of host
259 plants. Many fungal pathogens reduce survival, growth, and fecundity of host plants and lead
260 to the extinction of host populations. The detrimental effects of one pathogen on host plants
261 might have indirect effects on a second pathogen by reducing the number of intact host plants
262 and host populations available for the second pathogen to infect. Moreover, induced
263 resistance of hosts due to infection by one pathogen may reduce infection of second pathogen
264 (Hammerschmidt 1999). Whereas most previous studies have focused on pairwise
265 interactions (one host for one pathogen relationship, but see examples of double-infections by
266 plant viruses in Power 1996 and Syller 2012), multi-species host–pathogen systems, as we
267 have shown here, can provide new challenges for the understanding of ecology, evolution,
268 and biodiversity originating from host–pathogen dynamics.
269

270 **Disclosure**

271 The authors declare no conflict of interest. All the researches undertaken in this study comply
272 with the current laws of Japan.
273

274 **Acknowledgements**

We acknowledge the Sugadaira Montane Research Center (SMRC), University of Tsukuba, for permission to conduct research within the site. We also thank Yoshiaki Ideura, Mariko Kastuyama, Kouji Nagaoka, Ryuji Kanai, Takahiro Ogai, and Tsutomu Matsuzaki for their research assistance and a member of the SMRC for valuable advice regarding the field research.

References

Alexander H, Antonovics J, 1988. Disease spread and population dynamics of anther-smut infection of *Silene alba* caused by the fungus *Ustilago violacea*. *Journal of Ecology* 76: 91–104; dx.doi.org/10.2307/2260456.

Anderson PK, Cunningham AA, Patel NG, Morales FJ, Epstein PR, Daszak P, 2004. Emerging infectious diseases of plants: pathogen pollution, climate change and agrotechnology drivers. *Trends in Ecology and Evolution* 19: 535–544; dx.doi.org/10.1016/j.tree.2004.07.021.

Bardgett RD, Wardle DA, 2010. *Aboveground-belowground linkages: biotic interactions, ecosystem processes and global change*. Oxford University Press, New York.

Barot S, Gignoux J, Menaut J-C, 1999. Demography of a savanna palm tree: predictions from comprehensive spatial pattern analyses. *Ecology* 80: 1987–2005; dx.doi.org/10.2307/176673.

296 Brown JKM, Hovmøller MS, 2002. Aerial dispersal of pathogens on the global and
297 continental scales and its impact on plant disease. *Science* 297: 537–541;
298 dx.doi.org/10.1126/science.1072678.
299 Burdon JJ, Jarosz AM, Kirby GC, 1989. Pattern and patchness in plant-pathogen
300 interactions-causes and consequence. *Annual Review of Ecology and Systematics* 20:
301 119–136;
302 Burdon JJ, Ericson L, Müller WJ, 1995. Temporal and spatial changes rust pathogen
303 *Triphragmium ulmariae* and its host, *Filipendula ulmaria*. *Journal of Ecology* 83:
304 979–989; dx.doi.org/10.2307/2261179.
305 Burdon JJ, Thrall P, 1999. Spatial and temporal patterns in coevolving plant and pathogen
306 associations. *The American Naturalist* 153: S15–S33; dx.doi.org/10.1086/303209.
307 Cano C, Bago A, 2005. Competition and substrate colonization strategies of three
308 polyxenically grown arbuscular mycorrhizal fungi. *Mycologia* 97:1201–1214;
309 dx.doi.org/10.3852/mycologia.97.6.1201.
310 Carlsson-granér U, Thrall PH, 2002. The spatial distribution of plant populations, disease
311 dynamics and evolution of resistance. *Oikos* 97: 97–110;
312 dx.doi.org/10.1034/j.1600-0706.2002.970110.x.
313 Cole RG, Syms C, 1999. Using spatial pattern analysis to distinguish causes of mortality: an
314 example from kelp in north-eastern New Zealand. *Journal of Ecology* 87: 963–972;
315 dx.doi.org/10.1046/j.1365-2745.1999.00418.x.
316 Dale MRT, 1999. *Spatial pattern analysis in plant ecology*. Cambridge University Press,
317 Cambridge.

318 Daszak P, Cunningham AA, Hyatt AD, 2000. Emerging infectious diseases of
319 wildlife--threats to biodiversity and human health. *Science* 287: 443–449;
320 dx.doi.org/10.1126/science.287.5452.443.
321 Debski I, Burslem D, Palmiotto PA, Lafrankie JV, Lee HS, Manokaran N, 2002. Habitat
322 preferences of *Aporosa* in two Malaysian forests: Implications for abundance and
323 coexistence. *Ecology* 83:2005–2018;
324 dx.doi.org/10.1890/0012-9658(2002)083[2005:HPOAIT]2.0.CO;2.
325 Desprez-Loustau M-L, Robin C, Buée M, Courtecuisse R, Garbaye J, Suffert F, Sache I,
326 Rizzo DM, 2007. The fungal dimension of biological invasions. *Trends in Ecology and*
327 *Evolution* 22: 472–480; dx.doi.org/10.1016/j.tree.2007.04.005.
328 Dovčiak M, Frelich LE, Reich P, 2001. Discordance in spatial patterns of white pine (*Pinus*
329 *strobus*) size-classes in a patchy near-boreal forest. *Journal of Ecology* 89: 280–291;
330 dx.doi.org/10.1046/j.1365-2745.2001.00545.x.
331 Gadgil PD, 1984. *Cyclaneusma* (*Naemacyclus*) needle-cast of *Pinus radiata* in New Zealand.
332 1: Biology of *Cyclaneusma minus*. *New Zealand Journal of Forestry Science* 14:
333 179–196.
334 Garcia-Guzmaan G, Burdon JJ, Ash JE, Cunningham RB, 1996. Regional and local patterns
335 in the spatial distribution of the flower-infecting smut fungus *Sporisorium amphilophis*
336 in natural populations of its host *Bothriochloa macra*. *New Phytologist* 132: 459–469;
337 dx.doi.org/10.1111/j.1469-8137.1996.tb01866.x.
338 Hammerschmidt R (1999) Induced disease resistance : how do induced plants stop
339 pathogens ? Physiological and Molecular Plant Pathology 55: 77-84;
340 dx.doi.org/10.1006/pmpp.1999.0215

Hosoya T, Hosaka K, Saito Y, Degawa Y, Suzuki R, 2013. *Naemacyclus culmigenus*, a newly reported potential pathogen to *Miscanthus sinensis*, new to Japan. *Mycoscience*; doi.org/10.1016/j.myc.2013.02.002.

Kennedy PG, Bruns TD, 2005. Priority effects determine the outcome of ectomycorrhizal competition between two Rhizopogon species colonizing *Pinus muricata* seedlings. *New Phytologist* 166: 631–638; dx.doi.org/10.1111/j.1469-8137.2005.01355.x.

Kennedy PG, Hortal S, Bergemann SE, Bruns TD, 2007. Competitive interactions among three ectomycorrhizal fungi and their relation to host plant performance. *Journal of Ecology* 95: 1338–1345; dx.doi.org/10.1111/j.1365-2745.2007.01306.x.

Kennedy PG, 2010. Ectomycorrhizal fungi and interspecific competition: species interactions, community structure, coexistence mechanisms, and future research directions. *New Phytologist* 187: 895–910; dx.doi.org/10.1111/j.1469-8137.2010.03399.x.

Jennersten O, 1988. Insect dispersal of fungal disease: effects of *Ustilago* infection on pollinator attraction in *Viscaria vulgaris*. *Oikos* 51: 163–170; dx.doi.org/10.2307/3565638.

Laine A-L, 2004. Resistance variation within and among host populations in a plant -pathogen metapopulation: implications for regional pathogen dynamics. *Journal of Ecology* 92: 990–1000; dx.doi.org/10.1111/j.1365-2745.2005.01075.x.

Laine A-L, Hanski I, 2006. Large-scale spatial dynamics of a specialist plant pathogen in a fragmented landscape. *Journal of Ecology* 94: 217–226; dx.doi.org/10.1111/j.1365-2745.2005.01075.x.

Pélissier R, 1998. Tree spatial patterns in three contrasting plots of a southern Indian tropical moist evergreen forest. *Journal of Tropical Ecology* 14: 1–16;

dx.doi.org/10.1017/s0266467498000017.

Pickles BJ, Genney DR, Potts JM, Lennon JJ, Anderson IC, Alexander IJ, 2010. Spatial and temporal ecology of Scots pine ectomycorrhizas. *New Phytologist* 186: 755–768; dx.doi.org/10.1111/j.1469-8137.2010.03204.x.

Power A, 1996. Competition between viruses in a complex plant-pathogen system. *Ecology* 77: 1004–1010; dx.doi.org/10.2307/2265571.

Real LA, McElhany P, 2011. Spatial pattern and process in plant-pathogen interactions. *Ecology* 77: 1011–1025; dx.doi.org/10.2307/2265572.

Sakai AK, Oden NL, 1983. Spatial pattern of sex expression in silver maple (*Acer saccharnum* L.): Morisita's Index and spatial autocorrelation. *The American Naturalist* 122: 489–508; dx.doi.org/10.1086/284151.

Sokal RR, Oden NL, 1978a. Spatial autocorrelation in biology. I. Methodology. *Biological Journal of the Linnean Society* 10: 199–228; dx.doi.org/10.1111/j.1095-8312.1978.tb00013.x.

Sokal RR, Oden NL, 1978b. Spatial autocorrelation in biology. II. Some biological implications and four applications of evolutionary and ecological interest. *Biological Journal of the Linnean Society* 10: 229–249; dx.doi.org/10.1111/j.1095-8312.1978.tb00014.x.

Sterner RW, Ribic CA, Schatz GE, 1986. Testing for life historical changes in spatial patterns of four tropical tree species. *Journal of Ecology* 74: 621–633; dx.doi.org/10.2307/2260386.

Suzuki RO, Kudoh H, Kachi N, 2003. Spatial and temporal variations in mortality of the biennial plant, *Lysimachia rubida*: effects of intraspecific competition and

environmental heterogeneity. *Journal of Ecology* 91: 114–125; dx.doi.org/10.1046/j.1365-2745.2003.00745.x.

Suzuki RO, Suzuki J-I, Kachi N, 2005. Change in spatial patterns of a biennial plant between growth stages and generations in a patchy habitat. *Annuals of Botany* 96: 1009–1017.

Suzuki RO, Numata S, Okuda T, Nur Supardi MN, Kachi N, 2009. Growth strategies differentiate the spatial patterns of 11 dipterocarp species coexisting in a Malaysian tropical rain forest. *Journal of Plant Research* 122: 81–93; dx.doi.org/10.1007/s10265-008-0198-0.

Suzuki RO, Numata S, Okuda T, Nur Supardi MN, Abd Rahman K, Kachi,N, 2012. Species associations among dipterocarp species co-occurring in a Malaysian tropical rain forest. *Journal of Tropical Ecology* 28: 281–289.

Syller J, 2012. Facilitative and antagonistic interactions between plant viruses in mixed infections. *Molecular Plant Pathology* 13: 204–216; dx.doi.org/10.1111/j.1364-3703.2011.00734.x.

Thrall P, Burdon JJ, 1997. Host–pathogen dynamics in a metapopulation context: the ecological and evolutionary consequences of being spatial. *Journal of Ecology* 85: 743–753; dx.doi.org/10.2307/2960598.

Thrall P, Burdon JJ, 2000. Effect of resistance variation in a natural plant host–pathogen metapopulation on disease dynamics. *Plant Pathology* 49: 767–773; dx.doi.org/10.1046/j.1365-3059.2000.00523.x.

Thrall P, Burdon JJ, 2003. Evolution of virulence in a plant host-pathogen metapopulation. *Science* 299: 1735–1737; dx.doi.org/10.1126/science.1080070.

Webster J, Weber WS, 2007. *Introduction to fungi 3rd edn*. Cambridge University Press, New

410 York; dx.doi.org/10.1017/cbo9780511809026.

411

412

413 **Table 1** – Summary of the regional-scale census. The relative frequency was calculated as the
414 number of grid points with diseased plants divided by the number of grid points where host
415 plants were observed. Relative frequency was estimated based on a 5 × 5 grid-point census at
416 each site.

	Sites	Latitude	Longitude	Relative frequency of fungi	
				Sporisorium kusanoi	*Naemacyclus culmigenus*
1	Top of Minenohara ski slope	36° 33' 27. 44" N	138° 21' 33. 59" E	0	0
2	Mid of Minenohara ski slope	36° 33' 20. 71" N	138° 21' 25. 21" E	0.14	0
3	Minenohara park	36° 32' 58. 67" N	138° 21' 03. 10" E	0.5	0
4	Down of Minenohara ski slope	36° 33' 22. 17" N	138° 21' 09. 69" E	0.36	0
5	Dabos ski slope	36° 32' 04. 27" N	138° 20' 35. 51" E	0	0
6	Oomatsu ski slope course 1	36° 30' 54. 41" N	138° 18' 52. 79" E	0	0
7	Oomatsu ski slope course 2	36° 30' 56. 68" N	138° 18' 42. 98" E	0.08	0
8	SMRC	36° 31' 20. 13" N	138° 20' 54. 12" E	0.12	0.47 [a]
9	Oomatsu ski slope course 3	36° 31' 04. 17" N	138° 18' 39. 42" E	0	0
10	Tubakuro ski slope	36° 31' 44. 76" N	138° 18' 30. 09" E	0.24	0
11	Dabos hill	36° 32' 23. 75" N	138° 20' 54. 33" E	0.24	0

417 [a] Relative frequency of *N. culmigenus* at SMRC site was based on the local-scale census.

418

Figure legends

Fig. 1 – Maps showing 11 study sites (open circle) for the regional-scale census in the Sugadaira plateau region (**A**) and three 160-m transects (a in **B**) and a 60 × 100-m plot (b in **B**) for the local-scale census in Sugadaira Montane Research Center site (SMRC site). Number in **A** is corresponding to the site number in Table 1.

Fig. 2 – Seasonal changes in the prevalence of *Sporisorium kusanoi* (closed circle) and *Naemacyclus culmigenus* (open circle) on *Miscanthus sinensis*. The proportions of infected plots were calculated as the number of plots observed infected individuals divided by the number of plots observed *M. sinensis*.

Fig. 3 – Spatial distributions of (**A**) *Miscanthus sinensis*, (**B**) *Sporisorium kusanoi*, and (**C**) *Naemacyclus culmigenus.* These plants and pathogens were observed in closed areas.

Fig. 4 – Correlograms of Moran's *I* for (**A**) *Sporisorium kusanoi* and (**B**) *Naemacyclus culmigenus*, and (**C**) a correlogram of the cross-correlation (I_{12}) between the two fungi in July 2011. Moran's *I*s and I_{12} were calculated for distance classes with 1-m intervals. The solid line shows observed *I* values and broken lines indicate 99% confidence envelopes expected from the null hypothesis of random distribution (**A, B**) or spatial independence (**C**).

Figure

Fig. 1

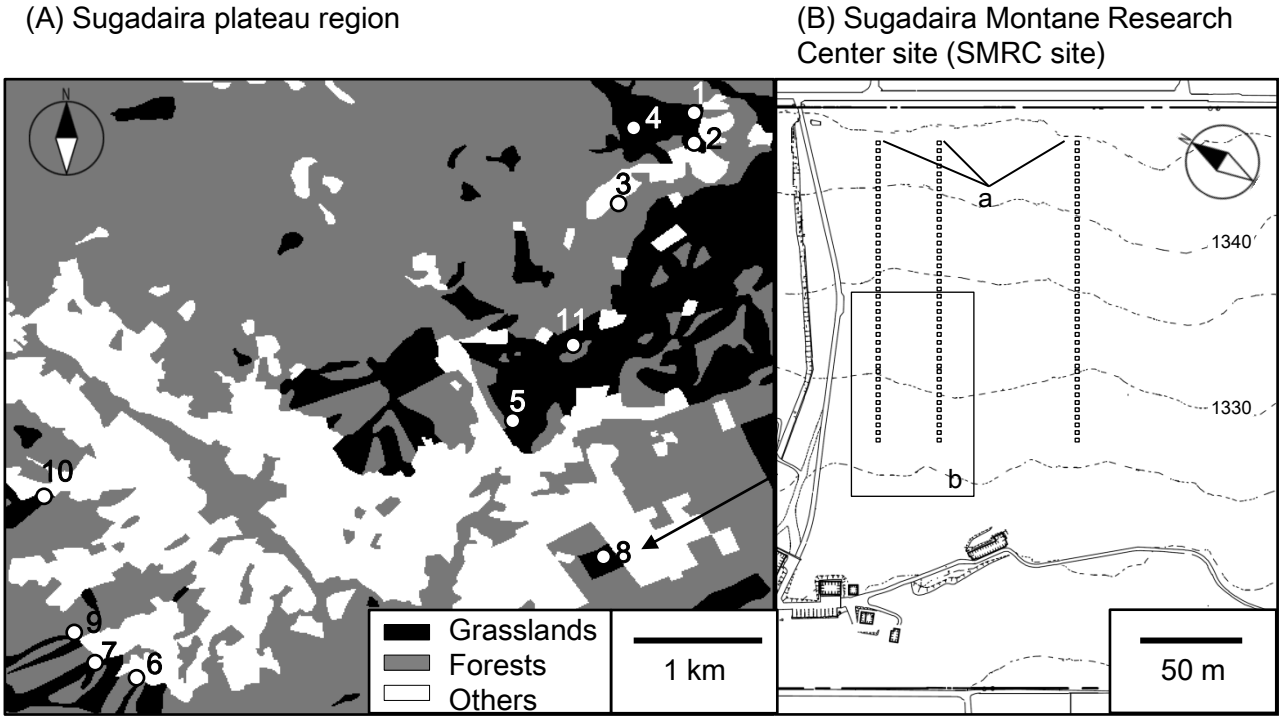
(A) Sugadaira plateau region
(B) Sugadaira Montane Research Center site (SMRC site)
N
1
2
3
4
5
6
7
8
9
10
11
Grasslands
Forests
Others
1 km
a
b
1340
1330
50 m

Fig. 2

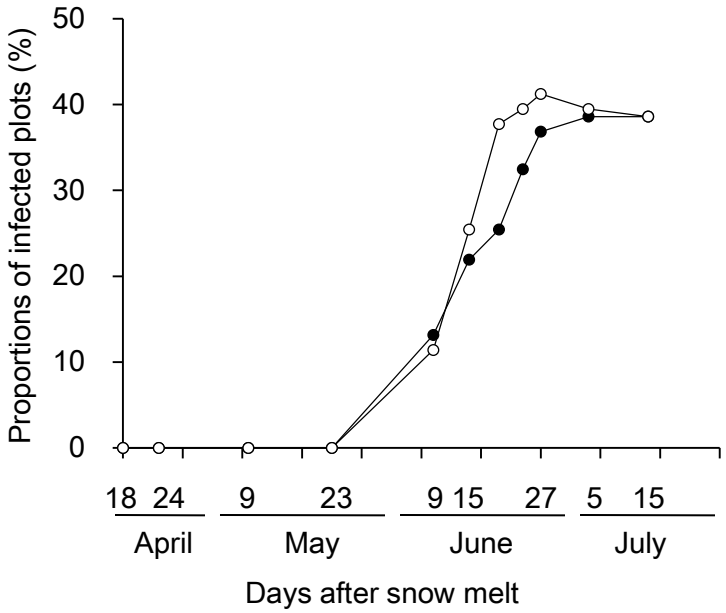
Proportions of infected plots (%)
50
40
30
20
10
0
18 24
9 23
9 15 27
5 15
April
May
June
July
Days after snow melt

Fig. 3

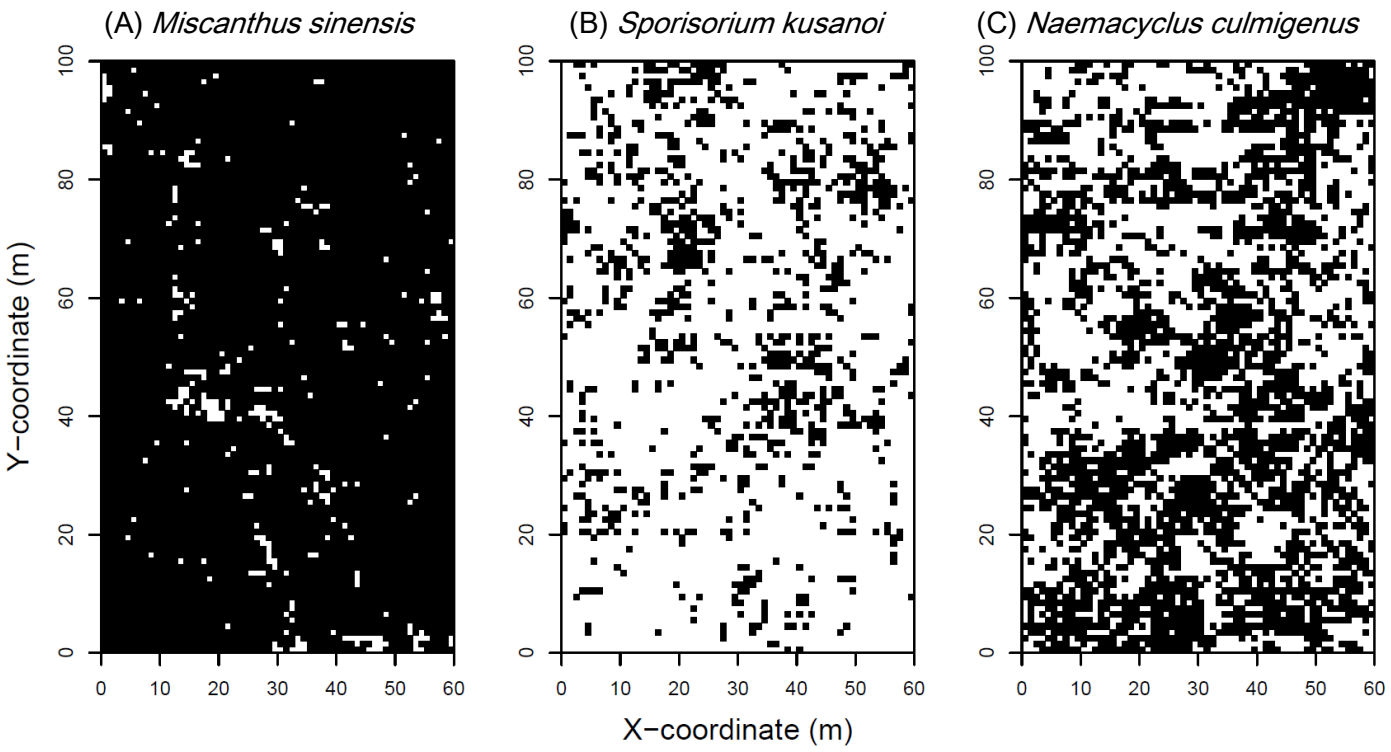
(A) Miscanthus sinensis
(B) Sporisorium kusanoi
(C) Naemacyclus culmigenus
Y−coordinate (m)
X−coordinate (m)
0
20
40
60
80
100
0
10
20
30
40
50
60

Fig. 4

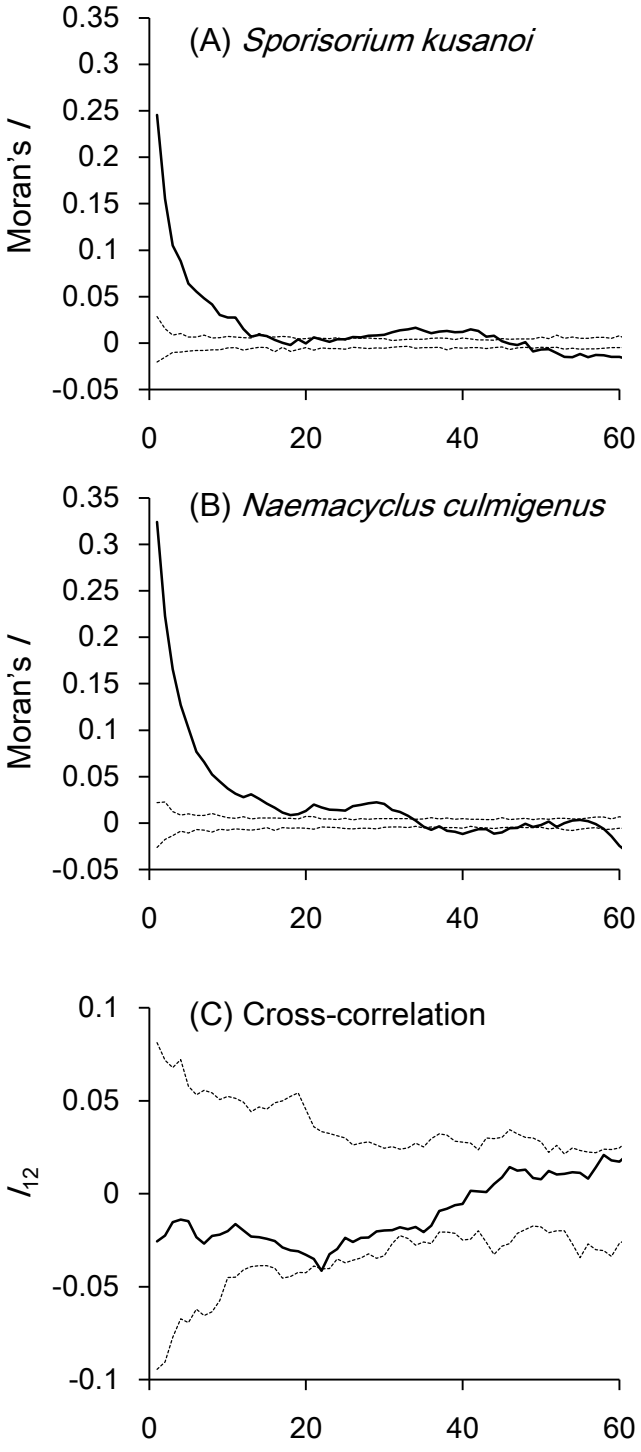
(A) *Sporisorium kusanoi*
Moran's *I*
0.35
0.3
0.25
0.2
0.15
0.1
0.05
0
-0.05
0
20
40
60
(B) *Naemacyclus culmigenus*
Moran's *I*
0.35
0.3
0.25
0.2
0.15
0.1
0.05
0
-0.05
0
20
40
60
(C) Cross-correlation
I_{12}
0.1
0.05
0
-0.05
-0.1
0
20
40
60

Highlights:

The spatio-temporal patterns in two pathogens of *Miscanthus sinensis* were revealed.

Sporisorium kusanoi was widely distributed within the region.

Naemacyclus culmigenus was restricted within a specific site.

The two fungi were observed in 17.2% and 47.3% subplots in the specific site.

Their disease symptoms emerged early in June and peaked early in July.